Influence of Different Material Models on the Result of Numerical High Speed Cutting Simulations*

Th. Halle[1], L. W. Meyer[2]

[1] Materials and Impact Engineering, Chemnitz University of Technology, Germany
[2] Chair Materials and Impact Engineering, Chemnitz Univ. of Technology,Germany

Abstract

Extreme conditions for the workpiece and the tool can occur in high speed cutting processes. Temperatures above 1000 °C at very high strains over 3 and strain rates near 105 1/s are not unusual. In the first part of this paper an overview about the well known and new developed testing methods for these extreme conditions is given. For numerical simulations it is necessary to formulate closed material models which include strain, strain rate, and the temperature.

In the second part some well known material models are presented and compared. Furthermore, advantages and disadvantages are named. The flow stress behaviour of two types of steel (1.1191, 1.2311) as a function of strain rate and temperature is presented. A Johnson-Cook and a Zerilli-Armstrong model is used for the comparative numerical simulations of an orthogonal cutting process. To indicate the process of chip segmentation, a damage model is often used. The influence of various damage models with different damage parameters and failure modes is shown. The calculated cutting forces and the shape of the chips are compared with results determined at a quickstop cutting device with integrated force measurement. Additionally, the calculated chip formation is compared with the measured shape by means of highspeed photography. The temperatures, forces, and chip shape for both used models are presented and the influence of different material models are evaluated and named.

Keywords:

Material, Modelling, Simulation

**This work is based on the results of DFG priority program "High Speed Cutting". The authors would like to thank the Deutsche Forschungsgemeinschaft (DFG) for their financial support.*

1 Introduction

For the simulation of High Speed Cutting processes, it is necessary to have reliable material data, friction data, and some other important variables. For highest accuracy of the FE-Simulation, these data measured should match the range of temperature, strain, and strain rate which occur in the machining processes. This paper gives a short overview of the devices to obtain this data and demonstrates the influence of material models on the simulation results. In order to describe the effect of different material data, all other variables, like friction, heat capacity, etc. are kept constant. Therefore, influence of friction and other parameters are not considered (see [1] for a description and reliable values of these parameters). In order to use constitutive equations of the Johnson/Cook- or Zerilli/Armstrong-type, the measured high rate adiabatic data have to be transferred into isothermal data.

2 Material and methods

In the case of High Speed Cutting (HSC) strain rates up to 2*105 do occur. To obtain the relevant material data, many researchers use the split Hopkinson pressure bar [2]. Depending on the specimen geometry, strain rates up to 20.000 1/s are possible. In the case of compression tests the maximum strain is about 0.5…0.6. The strain limit in tension testing is about 0,25, for high strength materials this value is reduced to 0,1 or less. Only with torsion tests it is possible to obtain flow stresses at very high strain rates and higher strains. In addition to the difficulty to measure flow stresses at high strain rates, it is essential to measure the flow behaviour at high temperatures up to 1000 °C. An overview of the possibilities to estimate material data at very high strain, temperatures, and strains is given in these proceedings by Meyer [3]. Therefore, in this paper only two devices developed for material testing at high strain rates and simultaneous high temperatures are named shortly.

2.1 Materials

Two steels C45E (1.1191) and 40CrMnMo7 (1.2311) were tested. The steel C45E is a quenched and tempered steel and is used in a wide range of technical

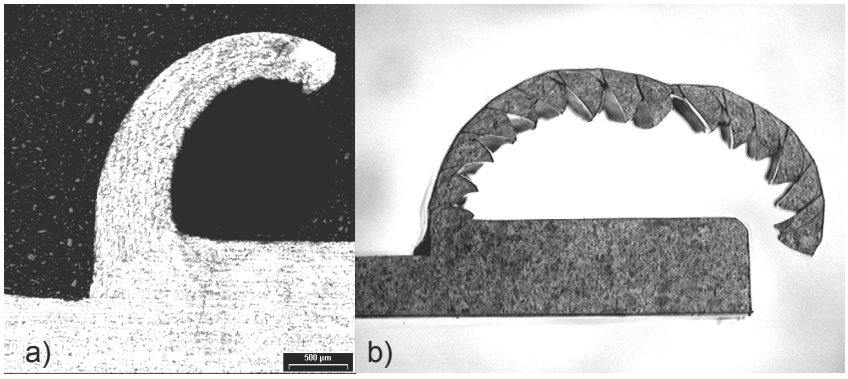

Figure 1: *a) continued chip C45 and b) segmented chip 40CrMnMo7 both obtained at a quick-stop device [4]*

applications. The steel 40CrMnMo7 is a tool steel and is often used for molds and dies. This material presents different chip shapes at HSC conditions. The C45E exhibits continuous chips up to high cutting speeds for cutting depths lower than 0.65 mm. In contrast to C45E the 40CrMnMo7 lead to chip segmentation (see Figure 1).

2.2 Testing Devices

In order to achieve highest strain rates, two testing devices were applied to measure the flow stress behaviour. For dynamic compression loading the split-Hopkinson-pressure-bar was used. High rate torsion loading was accomplished with a high speed torsion machine. Both test set-ups will be introduced briefly. For a closer look or other testing devices which can be used to determine high strain rate properties, the reader is reprehend to Meyer [3].

At the TUC the principle of SHPB is implemented in a rotating wheel which is described elsewhere [5]. The load is directly applied to the sample. A specification of the test set-up is presented in [6]. Tests up to strain rates of $10^4\ s^{-1}$ at temperatures above 1000°C are possible. However, flow curves up to relatively low strains of 0.05 to 0.15 can be obtained. For a simulation, flow stresses at higher strains are necessary. Therefore, a new type of torsion setup was developed in Chemnitz [3]. The principle is based on a direct loading of the torsion sample which is connected to a torsion Hopkinson bar. The machine is able to rotate up to 3000 rpm with no limitations regarding the rotating angle. This means, in dependence of the used specimen geometries, strain rates up to 10^4 1/s are possible.

2.3 Material Models

For the examination of the influence of various constitutive equations on the quality of the simulation, the models proposed by Johnson-Cook and Zerilli-Armstrong are used. Both models have a wide distribution to describe the flow stress behaviour of metallic materials. Especially the Johnson-Cook (JC) [7] model is often used for numerical simulations and is implemented in many implicit or explicit simulation tools. The Zerilli-Armstrong (ZA) [8] model is based on semi-empiric equations with respect to the mechanism of thermal activation [9].
The following equations represent the models of JC (Equation 1) and ZA (Equation 2, 3):

$$\sigma = \left(A + B\varepsilon^{n}\right)\cdot\left(1 + C\,ln\,\dot{\varepsilon}\right)\cdot\left[1 - \left(\frac{T - T_{room}}{T_{melt} - T_{room}}\right)^{m}\right] \tag{1}$$

$$\overset{krz}{\sigma} = \Delta\sigma_G + B_0\cdot exp\left[\left(-\beta_0 + \beta_1\,ln\,\dot{\varepsilon}\right)T\right] + k_0\varepsilon^{n} + k_\varepsilon\lambda^{-\frac{1}{2}} \tag{2}$$

$$\overset{kfz}{\sigma} = \Delta\sigma_G + B_0\cdot exp\left[\left(-\beta_0 + \beta_1\,ln\,\dot{\varepsilon}\right)T\right] + k_\varepsilon\lambda^{-\frac{1}{2}} \tag{3}$$

Both models have advantages and disadvantages to represent the “real” material. JC and also ZA are not able to describe the strain induced ageing. Both models can only describe a monotone decreasing flow stress with increasing temperatures. ZA and JC use an exponential approach. For JC (see Equation 1), only the “m” parameter describes the thermal softening behaviour of the modelled material. In the ZA model, three constants B_0, β_0

and β_1 have influence on the material softening. For this model, the softening behaviour is also dependent on the strain rate. As example for the C45E material in Figure 2, the influence of the used data pool on the fitting of the material parameters is explained. The used data pool of experimental tests is given by the following limits: strain rate between 0,0001 and 200.000 1/s, strain up to 4, and temperatures up to 1000°C. In the first case (see Figure 3a) only temperatures lower than 600°C were implemented in the data collection used to calculate the material parameters. A very good approximation, especially for the ZA model, with the measured data up to temperatures of 600°C is found. An extrapolation above temperatures of 200°C revealed a different performance of the ZA model and the JC model. The ZA model runs into saturation against the value of $\sigma_{sat} = \Delta\sigma_G + k_0\varepsilon^n$. On the other hand, if the JC Model is extrapolated beyond the fitting range the flow stresses decrease continuously. As a consequence, flow stresses lower than zero would be computed at higher temperatures. However, the "real" data are in good agreement up to 1000°C. Flow stresses lower than zero can lead to numerical

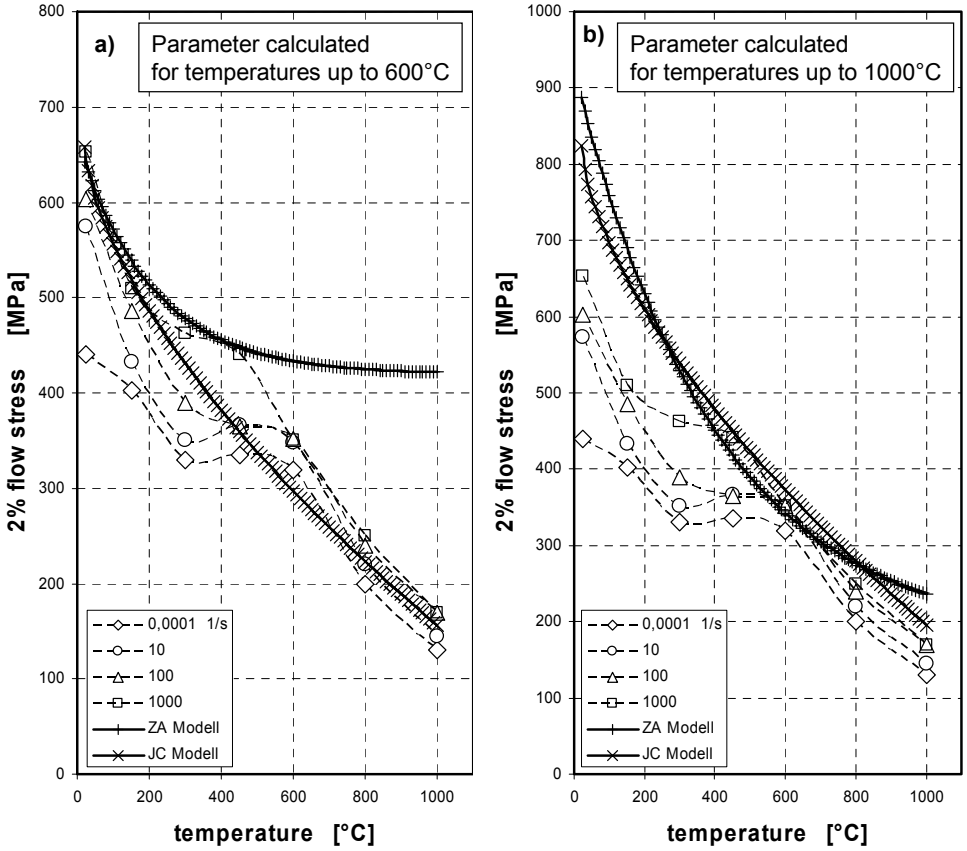

Figure 2: *Comparison of experimental data with ZA and JC models (both at a strain rate of 1000 1/s) by different data pools for fitting*

instabilities and incorrect results. On the other hand, the overestimated flow stresses by extrapolation of the ZA model lead to deviations by factors of about three at 1000°C. When the data pool for fitting the material parameters include tests at temperatures up to 1000°C, the progression presented in Figure 2b for ZA and JC is given. Both models overestimate the "real" material behaviour. Another important difference between the JC and the ZA model is the treatment to regard the strain rate. JC represents the strain rate

in a logarithmic scale in contrast to ZA, where the strain rate is represented by a double logarithmic scale. A linear increase in a logarithmic scale often does not represent the real material behaviour vs. the strain rate. Figure 3 illustrates this model behaviour in a dashed line for the steel C45E. Only the ZA model is able to calculate the progress of flow stresses vs. strain rate in a wide range of testing velocities. At very high strain rates the differences between the ZA and the JC model grow exponential. Therefore, it is concluded that an extrapolation above the given limits, especially to higher temperatures, is problematic. Numerical instabilities or flow stress values above factor 2 or higher compared with the "real" material behaviour are possible. Both models show in some areas relatively great differences to the experimental values. The question is: How important is the used material model for the quality of a numerical simulation of an orthogonal high speed cutting process?

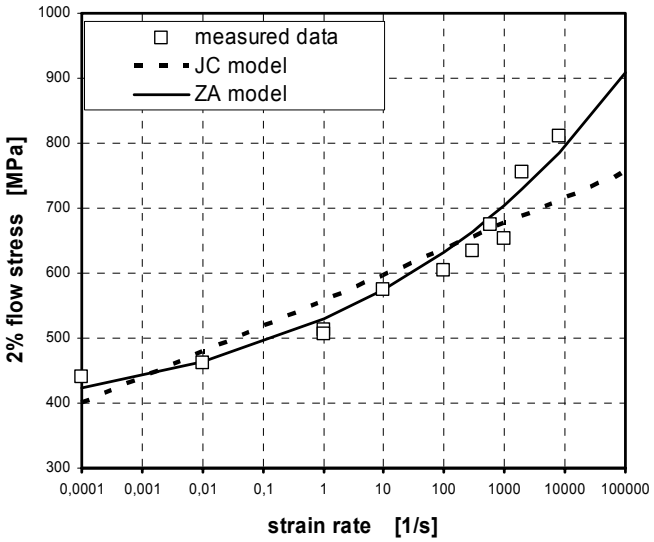

Figure 3: *Experimental data and fitting by the ZA and the JC model versus the strain rate under tensile loading of steel C45*

3 Results

3.1 Numerical Simulations

All following presented numerical simulations accord to a quick-stop device with integrated force measurement and high speed photography. This device was described in [4]. For all simulations, the FE-Program DEFORM® in 2D was used. In 3D some imported program features like self contact are not implemented yet. To obtain the influence of different material or failure models, the following approached boundary conditions are used: an orthogonal cutting process with a cutting speed of 600 m/min, a chip angle of 0°, and a free angle of 6°. In all cases the friction was assumed as shear type with a constant value of 0.3. Three possibilities to incorporate the flow stress data were used. Firstly, the measured data were transferred carefully into piecewise (PW) isothermal curves. In both other cases the experimental data were transferred into a Johnson-Cook (JC) and a Zerilli-Armstrong (ZA) model. The parameter calculation for both models was made without any constrains for the parameters to receive a high coefficient of determination r^2.

Both models are not available in the 2D Version of the used FE-Code. Therefore, it was necessary to implement both models as flow stress routines into the code. This was realised by writing two FORTRAN subroutines. For these routines, the equation 1 and also the both derivations w.r.t. strain (equation 4) and strain rate (equation 5) were used to formulate the Johnson-Cook model. In the same way the Zerilli-Armstrong model was implemented by using the equations 2, 6 and 7.

$$\frac{d\sigma}{d\varepsilon} = \left(1 + C\,ln\,\dot{\varepsilon}\right)\cdot\left[1-\left(\frac{T-T_{room}}{T_{melt}-T_{room}}\right)^{m}\right]\cdot\frac{Bn}{\varepsilon}\varepsilon^{n} \tag{4}$$

$$\frac{d\sigma}{d\dot{\varepsilon}} = \left(A + B\varepsilon^{n}\right)\cdot\left[1-\left(\frac{T-T_{room}}{T_{melt}-T_{room}}\right)^{m}\right]\cdot C\frac{1}{\dot{\varepsilon}} \tag{5}$$

$$\frac{d\sigma}{d\varepsilon} = \frac{nk_0\varepsilon^{n}}{\varepsilon} \qquad \text{when n<1} \tag{6}$$

$$\frac{d\sigma}{d\dot{\varepsilon}} = \frac{B_0\beta_1 T}{\dot{\varepsilon}\cdot exp\left(\beta_0 T\right)}exp\left(\beta_1 T\,ln\,\dot{\varepsilon}\right) \tag{7}$$

For the failure model evaluation, eleven different failure models are used.

3.2 Comparison of different material models for steel 1.1191

To evaluate the influence of a material model, calculations in a wide range of cutting speeds and cutting depths were performed. The ascertained deviations between the three used data pools are generally not large. Representative for all calculations a simulation of 600 m/min with a cutting depth of 0.5 mm is shown.

In Figure 4 the differences between the models for the maximum of temperature, strain, strain rate, and the cutting force are presented. The shown values are determined at a path along the calculated chip surface. The deviations for all values are relatively small. The values for the calculated temperatures and cutting forces vary at about 5% and decrease a little bit with increasing cutting depth and increase with decreasing cutting speed. For the maximum equivalent strain and the strain rate, the results vary about 10-20%. These results demonstrate that both models can be used instead of piecewise data in numerical simulations of high speed cutting processes without generating large errors. Especially for cutting force calculations the error generated by using a material model is smaller than 5%.

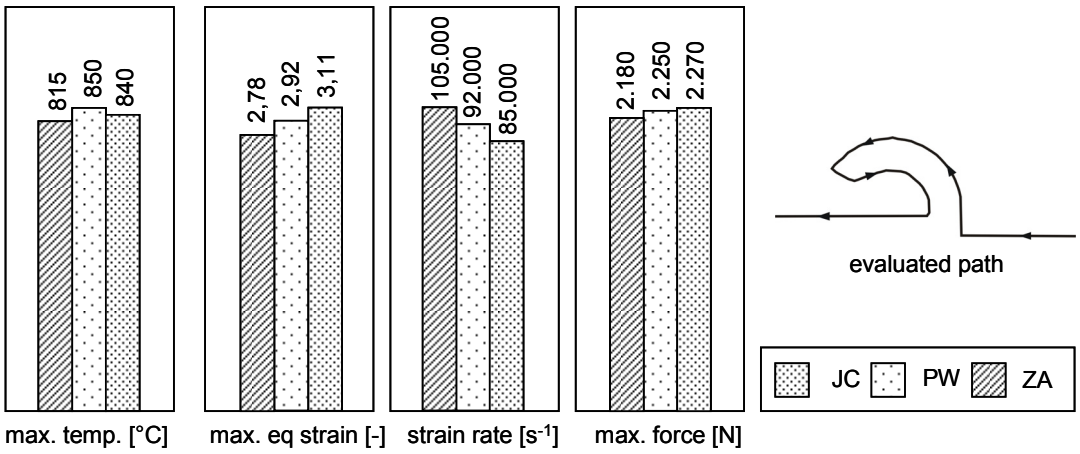

Figure 4: *Influence of different material models on simulation results*

The effects of different models on the computed chip shape are presented in Figure 5. Simulated was a quick-stop test with a cutting path of 7 mm. After a cutting distance of 2 mm all three simulations reveal nearly the same chip geometry. With increasing cutting distance the influence of the used models grows. This leads to a self contact at 6.5 mm distance of cutting for the ZA model. The PW simulation gives the best match with the experimental results (see chapter 3.4). Nevertheless, the other material models are very close to these results.

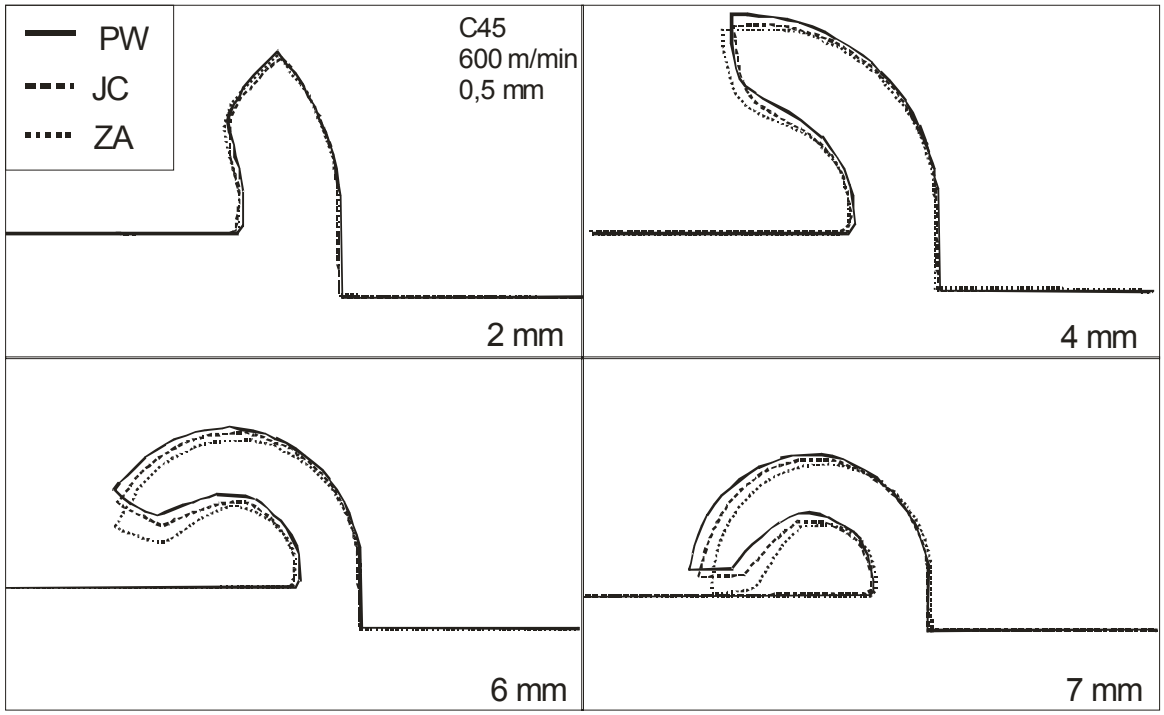

Figure 5: *Chip shape simulation results for PW, JC and ZA input data with increasing path of cutting.*

3.3 Comparison of different failure models for steel 1.2311

In addition to the simulations with different flow stress models, some calculations with varied failure models were executed with the tool steel 1.2311. The material data for 1.2311 are used by PW data. In a first step, calculations with failure parameters according to literature data or estimated parameter without element deletion are computed. These simulations are performed to estimate the critical values for each of the eleven tested models. In a second step, an element deletion for these calculations is used and the calculations were started again. All simulations stop due to numerical instabilities and the last simulation step of this procedure is presented in Figure 6.

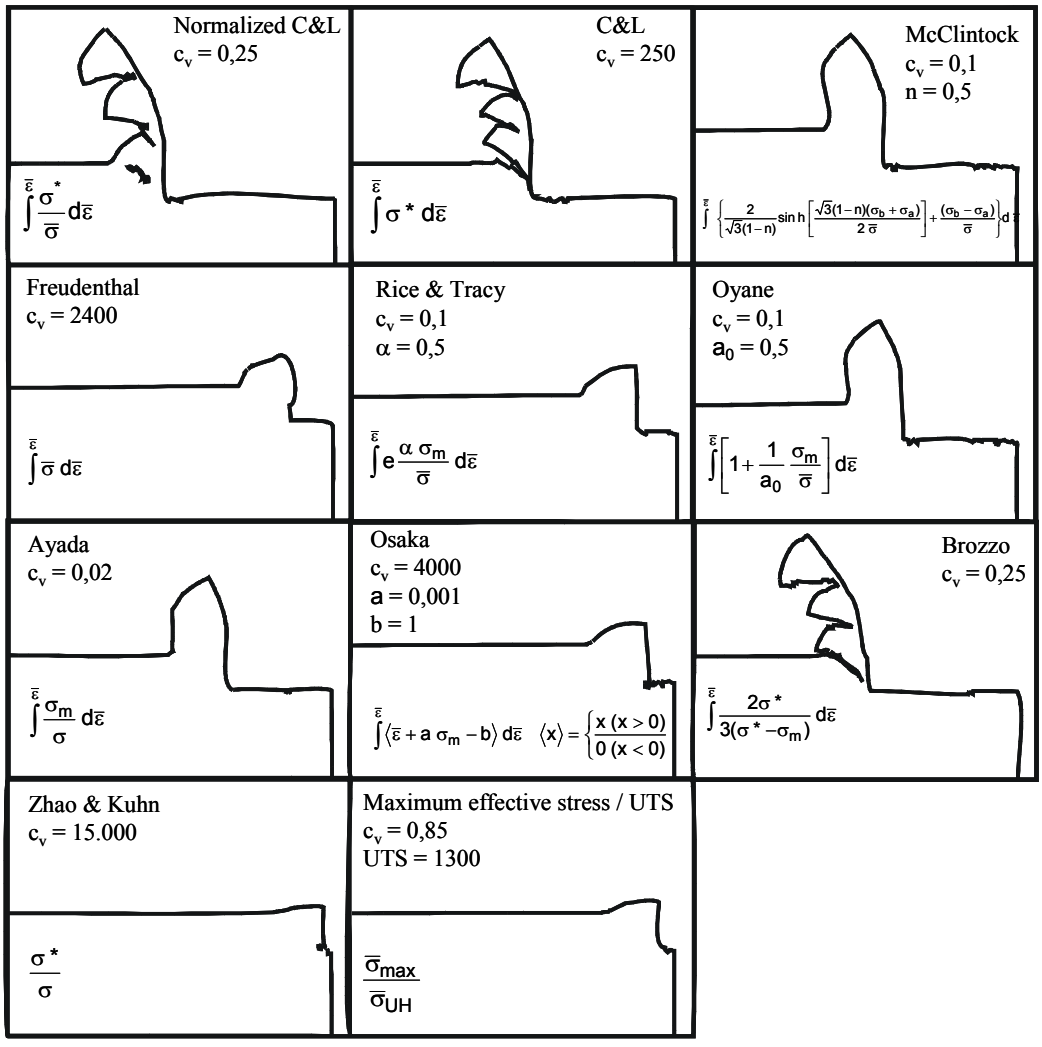

Figure 6: *Chip shape simulation results different failure models at 1.2311*

For the used simple approach only three models are able to reach a macroscopic match with the experimental cutting results (see Figure 1). The adiabatic shear instability, which occurs in reality, can not be obtained with the used simulation configuration.

3.4 Comparison of experimental and simulation results

To demonstrate the good geometry match between numerical simulations and experimental results, a comparison of an obtained chip formation process is shown in Figure 7. A picture series was taken during a quick-stop-test at the C45E material with a cutting depth of 0.76 mm. A Imacon® highspeed CCD Camera with a macro lens was used. These pictures have a time resolution between each picture of 0.08 ms. Over these pictures the calculated chip shape at the same time step is laid. For further analyses with the concept of visioplasticity, a grid is upset on the material surface. Up to 5 mm distance of cutting a good match between calculated and the real experiment is visible. The simulation calculates cutting forces in the range (± 10%) of the measured forces obtained at the quick-stop-device. In addition, the calculated temperatures are slightly overestimated compared with the high rate experimental data [10]. Temperatures of approximately 800°C were measured. The compression of the chip is overestimated. This means that the real chip is thinner and slightly longer. Also the shear angle is not exact the same value like in the numerical simulation.

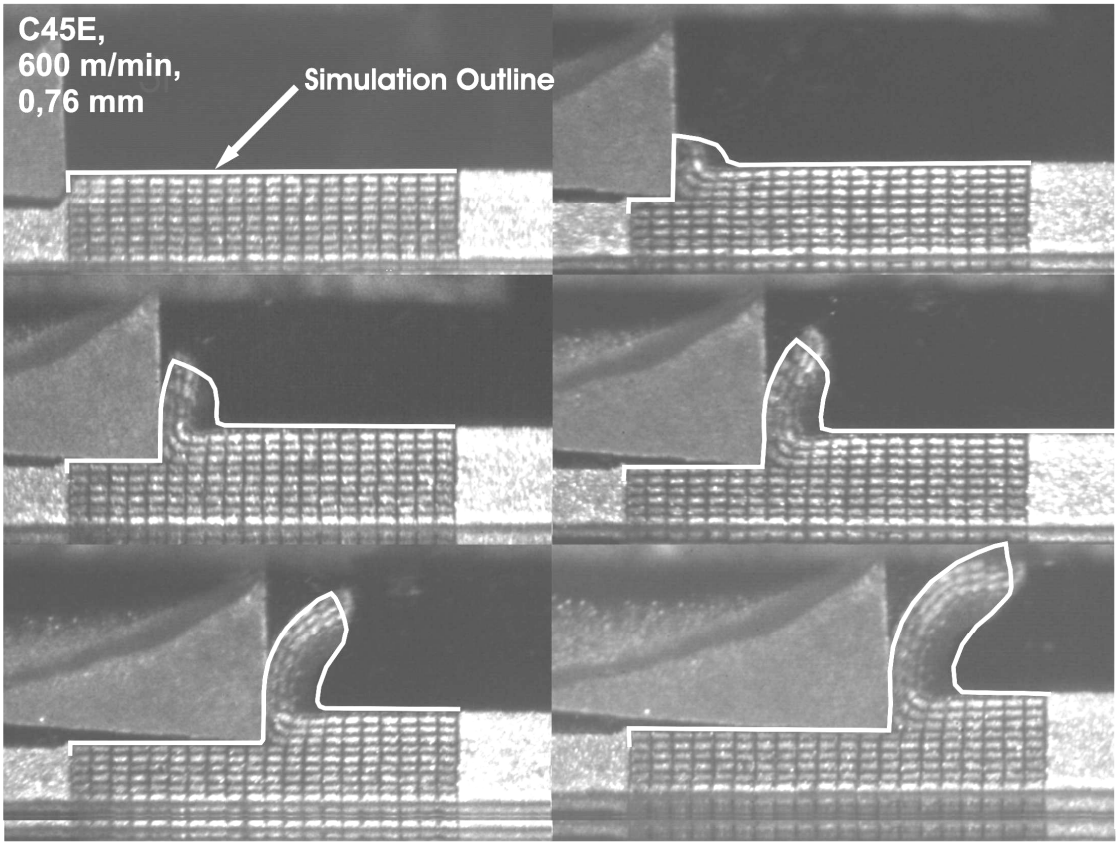

Figure 7: *Comparison of computed chip shape contours with pictures obtained with high speed photography at a quick-stop test*

4 Conclusions

The influence of material models on the results of high speed cutting simulations is evaluated and leads to deviations between 5 and 20%. Especially for determining the cutting forces for a tool analysis it is regardless which kind of material model is used. The ZA and the JC model can deliver good results in relation to the quality of the measured material data. It seems that only three of the used failure models are able to represent the macroscopic segmentation behaviour for the chip formation of the 1.2311 tool steel.

References

[1] *Boisse, P.; Altan, T.; Luttervelt, K. van.:* Friction and flow stress in forming and cutting, Kogan Page Science, 2003, ISBN 1-9039-9641-4.

[2] *(Rusty) Gray III, G.T.:* Classic Split-Hopkinson Pressure Bar Testing. Mechanical Testing and Evaluation. ASM International, Materials Park, Ohio, 2000, p.462-476., 10th ed. Handbook No.8.

[3] *Meyer, L.W.:* Material Behaviour at High Strain Rates. Proceedings of "1st International Conference on High Speed Forming", Dortmund, 2004.

[4] *Meyer, L.W.; Hahn, F.; Halle, T.:* Gestoppte Span- und Zugversuche - Schädigungsentwicklung und –fortschritt. Proceedings of "Werkstoffprüfung 2000", Bad Nauheim, 2000, p.323-333. DVM.

[5] *Meyer, L.W.; Halle, T.; Abdel-Malek, S.:* Tensile Testing, ASM International, Materials Park, Ohio, 2000, p.452-454. 10th ed. Handbook No.8.

[6] *Meyer, L.W.; Halle, T.:* Schlagdynamisches Werkstoffverhalten der Stähle C45E und 40CrMnMo7 bei erhöhten Temperaturen und hohen Dehngeschwindigkeiten unter Zugbeanspruchung. Proceedings of "Werkstoffprüfung 2000", Bad Nauheim, 2000, p.349-358.

[7] *Johnson, G.R.; Cook, W.H.:* A Constitutive Model and Data for Metals Subjected to Large Strains, High Strain Rates and High Temperatures. Proceedings of "7th Symposium on Ballistics", 1983, p.541-547.

[8] *Zerilli, F.J.; Armstrong, R.W.:* Constitutive Relations for the Plastic Deformation of Metals. American Institute of Physics, 1994, p.989-992.

[9] *Vöhringer, O.:* Effect of Temperature and Strain Rate on the Deformation Behaviour at Uniaxial Loading of Metallic Materials. Microstructure and Mechanical Properties of Materials, DGM Informationsgesellschaft mbH, Oberursel, 1991, p.41-50.

[10] *Frohmüller, R.:* Entwicklung, Aufbau und Funktionserprobung von Strahlmesstechnik zur Messung der Temperaturen in der Wirkzone bei hochdynamischen Zerspanvorgängen, Otto-von-Guericke-Universität Magdeburg, thesis, 2002.